RESEARCH ARTICLE

CLIMATE CHANGE

The oceanic sink for anthropogenic CO_2 from 1994 to 2007

Nicolas Gruber[1]*, Dominic Clement[1], Brendan R. Carter[2,3], Richard A. Feely[2], Steven van Heuven[4], Mario Hoppema[5], Masao Ishii[6], Robert M. Key[7], Alex Kozyr[8], Siv K. Lauvset[9,10], Claire Lo Monaco[11], Jeremy T. Mathis[12], Akihiko Murata[13], Are Olsen[10], Fiz F. Perez[14], Christopher L. Sabine[15], Toste Tanhua[16], Rik Wanninkhof[17]

We quantify the oceanic sink for anthropogenic carbon dioxide (CO_2) over the period 1994 to 2007 by using observations from the global repeat hydrography program and contrasting them to observations from the 1990s. Using a linear regression–based method, we find a global increase in the anthropogenic CO_2 inventory of 34 ± 4 petagrams of carbon (Pg C) between 1994 and 2007. This is equivalent to an average uptake rate of 2.6 ± 0.3 Pg C $year^{-1}$ and represents 31 ± 4% of the global anthropogenic CO_2 emissions over this period. Although this global ocean sink estimate is consistent with the expectation of the ocean uptake having increased in proportion to the rise in atmospheric CO_2, substantial regional differences in storage rate are found, likely owing to climate variability–driven changes in ocean circulation.

Using observations from the first global survey of inorganic carbon in the ocean conducted as part of the World Ocean Circulation Experiment (WOCE)–Joint Global Ocean Flux Study (JGOFS) programs during the 1980s and early 1990s, Sabine *et al.* (*1*) estimated that the ocean has taken up 118 ± 18 Pg (1 Pg = 10^{15} g) of anthropogenic carbon, C_{ant}, from the atmosphere from the beginning of the industrial revolution to the mid-1990s. Anthropogenic carbon represents the additional inorganic carbon present in the ocean-atmosphere system as a consequence of human emissions to the atmosphere (*2*, *3*) through the burning of fossil fuel, the production of cement, and land-use change (*4*, *5*). We distinguish this anthropogenic component from the fluxes and storage changes associated with natural CO_2, i.e., the quantity of carbon in the atmosphere-ocean system that existed already in preindustrial times (*6*). Here, using newly developed methods and high-quality ocean observations collected since 2003 on repeat hydrographic cruises (*7*), we extend the analysis of Sabine *et al.* (*1*) to 2007. In particular, we reconstruct the increase in the oceanic storage of C_{ant} between 1994 and 2007 and contrast this to the expected change given the continued increase in atmospheric CO_2.

Detecting the change in anthropogenic CO_2

We use the data synthesized by the Global Ocean Data Analysis Project version 2 (GLODAPv2) (*8*) and the recently developed eMLR(C*) method (*9*) to identify the change in C_{ant} (Δ_tC_{ant}) between the WOCE-JGOFS (nominal 1994) and the Repeat Hydrography–GO-SHIP (nominal 2007) periods (see supplementary materials for details, figs. S3 to S5). This method builds on the extended multiple linear regression (eMLR) approach (*10*), which was designed to separate Δ_tC_{ant} from any natural CO_2-driven change in dissolved inorganic carbon. The eMLR(C*) method has been extensively tested with synthetic data from a biogeochemical model (*9*), demonstrating its ability to reconstruct Δ_tC_{ant} with high accuracy at global and basin scales. These tests also revealed that subbasin scales are less well resolved, especially in regions characterized by high temporal variability. To quantify the uncertainties in the reconstructions, we used the spread from a Monte Carlo analysis and an ensemble of 14 sensitivity studies (see supplementary materials for details).

Global distribution

The global, vertical distribution of Δ_tC_{ant} between 1994 and 2007 reveals the strong gradients that are characteristic for a passive conservative tracer invading the ocean from the surface (Fig. 1). In the upper 100 m, C_{ant} increased, on average, by 14 μmol kg^{-1} over this period, close to the expected level given the rise in atmospheric CO_2 and the ocean's buffer capacity (*11*). Below that, Δ_tC_{ant} decreases rapidly with depth, reaching half of the surface value at 375 m and $^1/_{10}$ of it at 1000 m. Half of the global Δ_tC_{ant} signal is found in the top 400 m, more than 75% above 1000 m, and only about 7% between 2000 and 3000 m.

There are strong spatial variations in the vertical penetration of Δ_tC_{ant} (Fig. 1), reflecting the differences in the efficacy with which the surface signal is transported and mixed down by the large-scale overturning circulation (*1*, *3*, *12*–*14*). As transport occurs primarily along sloping neutral density surfaces (*15*), it is instructive to investigate the distribution of Δ_tC_{ant} on such iso-surfaces (Fig. 2). The relatively shallow surfaces associated with mode waters (such as the neutral surface 26.60 kg m^{-3}) (*16*) are ventilated on time scales of a few decades or less, such that the anthropogenic CO_2 signal is transported rather effectively from the outcrops at the mid to high latitudes toward the ocean's interior (Fig. 2A). By contrast, substantial changes in C_{ant} on the deeper (~1000 m in the mid and low latitudes) 27.40 kg m^{-3} neutral surface are essentially limited to the regions close to the outcrop (Fig. 2B). This reflects the decade- to century-long ventilation ages of the water masses occupying this neutral surface, consisting, in the Southern Hemisphere, primarily of Antarctic Intermediate Water. Despite its limited horizontal reach, the downward transport of the Δ_tC_{ant} signal along this neutral surface from the Southern Ocean outcrop leads to the second-deepest penetration of Δ_tC_{ant} anywhere in the ocean (Fig. 1). The deepest penetration is found in the North Atlantic, where the downward spreading of newly formed North Atlantic Deep Water (NADW) causes a Δ_tC_{ant} with a maximum of 5 μmol kg^{-1} below 1000 m. The rapid southward spreading of NADW between about 1500 and 2500 m transports this elevated Δ_tC_{ant} into the South Atlantic. The corresponding process is much less vigorous and deep-reaching in the North Pacific, as there is no deep-water formation there. This leads to a shallow penetration by mode and intermediate waters.

These regional differences in the vertical penetration cause large spatial variations in the column inventory of Δ_tC_{ant}, i.e., the change in C_{ant} integrated vertically from the surface down to 3000 m (Fig. 3A). Large parts of the mid-latitude North Atlantic increased their anthropogenic CO_2 loads by 16 ± 1 mol C m^{-2} or more between 1994 and 2007. This corresponds to an average

[1]Environmental Physics, Institute of Biogeochemistry and Pollutant Dynamics, ETH Zurich, Zurich, Switzerland. [2]National Oceanic and Atmospheric Administration, Pacific Marine Environmental Laboratory, Seattle, WA, USA. [3]Joint Institute for the Study of the Atmosphere and Ocean, University of Washington, Seattle, WA, USA. [4]Centre for Isotope Research, Faculty of Science and Engineering, University of Groningen, Groningen, Netherlands. [5]Alfred Wegener Institute, Helmholtz Centre for Polar and Marine Research, Bremerhaven, Germany. [6]Meteorological Research Institute, Japan Meteorological Agency, Tsukuba, Japan. [7]Atmospheric and Oceanic Sciences, Princeton University, Princeton, NJ, USA. [8]NOAA National Centers for Environmental Information, Silver Spring, MD, USA. [9]NORCE Norwegian Research Centre, Bjerknes Centre for Climate Research, Bergen, Norway. [10]Geophysical Institute, University of Bergen and Bjerknes Centre for Climate Research, Bergen, Norway. [11]LOCEAN, CNRS, Sorbonne Université, Paris, France. [12]National Oceanic and Atmospheric Administration, Arctic Research Program, Silver Spring, MD, USA. [13]Research and Development Center for Global Change, Japan Agency for Marine-Earth Science and Technology, Yokosuka, Japan. [14]Instituto de Investigaciones Marinas, CSIC (IIM-CSIC), Vigo, Spain. [15]Department of Oceanography, University of Hawai`i at Manoa, Honolulu, HI, USA. [16]GEOMAR Helmholtz Centre for Ocean Research Kiel, Kiel, Germany. [17]National Oceanic and Atmospheric Administration, Atlantic Oceanographic and Meteorological Laboratory, Miami, FL, USA.
*Corresponding author. Email: nicolas.gruber@env.ethz.ch

storage rate of 1.2 ± 0.1 mol m^{-2} $year^{-1}$; twice the global mean storage rate of 0.65 ± 0.08 mol m^{-2} $year^{-1}$. Large changes are also found along a broad zonal band in the mid-latitudes of the Southern Hemisphere, with maximum values above 15 ± 2 mol m^{-2} throughout much of the South Atlantic, and progressively smaller values going eastward into the Indian and Pacific Oceans. This reflects the deep, but spatially variable, penetration of C_{ant} into the thermoclines of these basins induced by downward transport by mode and intermediate waters (*17*, *18*) (compare Fig. 1), i.e., the upper cell of the meridional overturning circulation in the Southern Hemisphere (*19*).

In contrast to the regions with high accumulation, the low column inventory changes in the region south of 60°S stand out. The average change in storage there is less than 4 ± 2 mol m^{-2}, corresponding to a rate of only 0.30 ± 0.15 mol m^{-2} $year^{-1}$, i.e., less than half of the global mean. This low storage rate is associated with the lower cell of the meridional overturning circulation (*19*). First, the upwelling of old waters with low concentrations of C_{ant} (compare Fig. 1) around the Antarctic Polar Front prevents a substantial accumulation of C_{ant} there. Second, there is little downward transport associated with the downward component of the lower cell, likely owing to the physical blocking of the air-sea exchange of CO_2 by sea ice in the Antarctic zone and the relatively short residence time of these waters at the surface (*20*). This contrasts strongly with the upper overturning cell, which takes up a lot of anthropogenic CO_2 from the atmosphere but quickly transports it northward into the band of high storage between 50°S and 30°S (*14*, *17*, *21*).

Global and regional inventory change

Integrated globally and down to a depth of 3000 m, we estimate a change in the inventory of oceanic anthropogenic CO_2 of 31.2 ± 4 Pg C for the period 1994 to 2007 (Table 1 and table S3). To this we add the uptake and storage by regions outside our gridded domain, namely, the Mediterranean Sea and the Arctic Ocean, which are estimated to account for ~1.5 Pg C (*22*–*24*). We add an additional ~1 Pg C to our estimate to account for the accumulation of C_{ant} below 3000 m, estimated from the fraction of C_{ant} found below that depth in 1994 in the observational estimates (*1*) [see also (*25*)] and from the fraction modeled for the 1994 to 2007 period (*14*). This yields a global oceanic storage increase of anthropogenic CO_2 of 34 ± 4 Pg C, which equals a mean annual uptake rate of 2.6 ±0.3 Pg C $year^{-1}$ over the 1994 to 2007 period.

The individual ocean basins and hemispheres contribute very differently to both the global inventory and its uncertainty (Table 1). Between the hemispheres, the majority (60 ± 11%) of the increase in C_{ant} is found in the Southern Hemisphere (Table 1). Between the basins, the storage in the Pacific (39 ± 4%) and Atlantic (35 ± 4%) has increased by roughly equal amounts, whereas the contribution of the Indian Ocean is much smaller (21 ± 10%). Although this smaller storage in the Indian ocean reflects its fractional area coverage, the areal storage in the Atlantic is nearly twice that in the Pacific, primarily reflecting the differences in the uptake and downward transport in the high northern latitudes of these two basins. The largest uncertainty stems from the Indian Ocean, primarily as a result of the poor data coverage since 2000 (fig. S1B).

Adding the 34 ± 4 Pg C increase between 1994 and 2007 to the 118 ± 19 Pg C estimated for the change between the preindustrial period and 1994 (*1*) yields a global ocean storage for 2007 of 152 ± 20 Pg C. Extrapolating this estimate linearly to the year 2010 gives an inventory of 160 ± 20 Pg C, which is consistent with the "best" estimate provided by Khatiwala *et al.* (*13*) of 155 ± 31 Pg C, obtained by combining models and other constraints. Our estimate confirms also the results of a recent diagnostic model

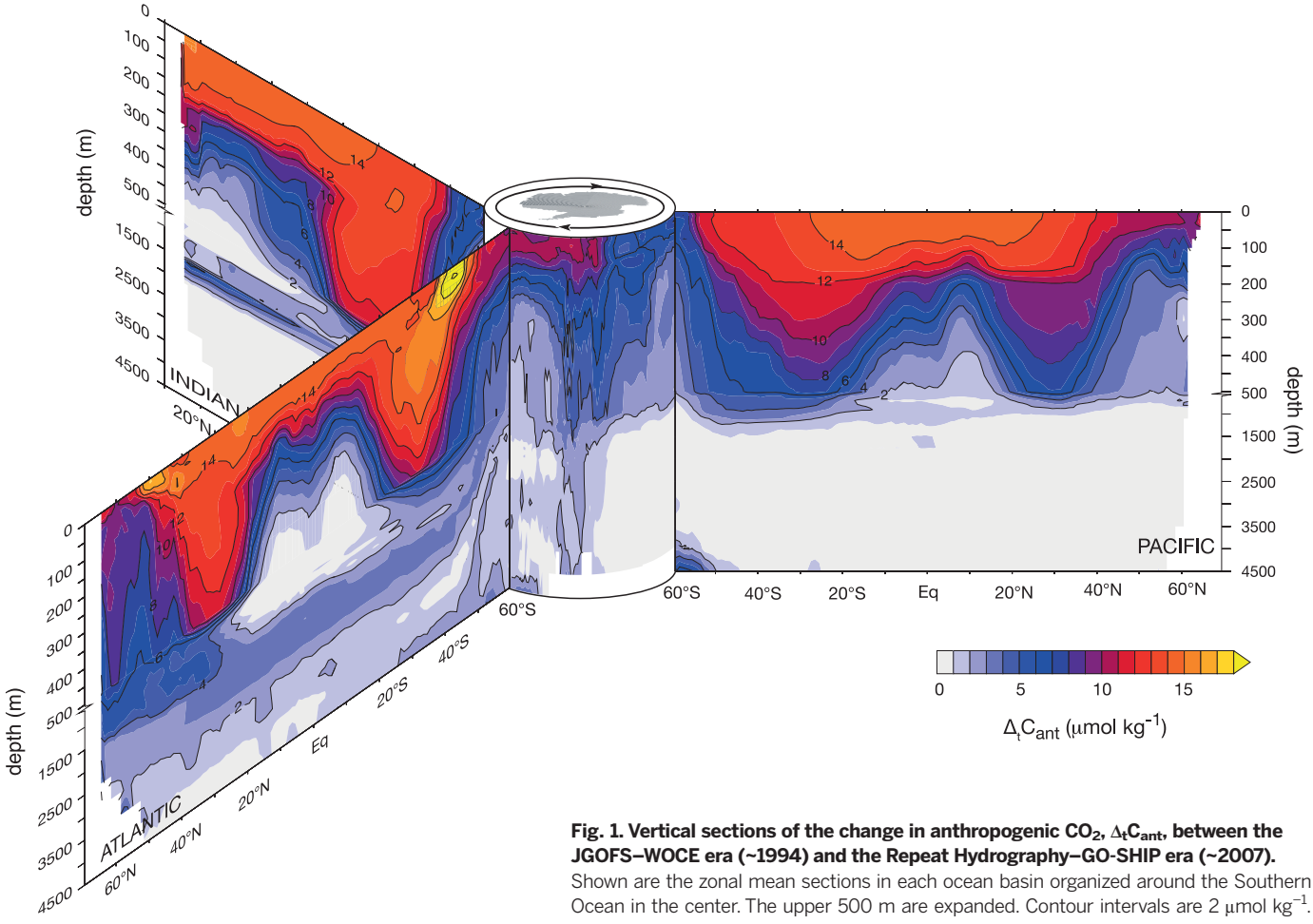

Fig. 1. Vertical sections of the change in anthropogenic CO_2, $\Delta_t C_{ant}$, between the JGOFS–WOCE era (~1994) and the Repeat Hydrography–GO-SHIP era (~2007). Shown are the zonal mean sections in each ocean basin organized around the Southern Ocean in the center. The upper 500 m are expanded. Contour intervals are 2 μmol kg^{-1}.

(*14*), which simulated a cumulative storage of about 155 to 161 Pg C for 2010. Our estimate stands out by its use of inorganic carbon measurements as the foundation to determine anthropogenic CO_2 inventories, whereas the other referenced studies employed indirect or model-based methods. Our approach also implicitly includes the effect of a time-changing ocean circulation, whereas the indirect estimates of (*14*, *26*) assume a steady-state ocean circulation.

The eMLR(C*)-based estimates of Δ_tC_{ant} compare overall well with other regional data-based analyses of the change in anthropogenic CO_2 conducted so far, both in terms of the vertical distributions and the column inventories (see supplementary materials). Our data-based storage rates for the period 1994 to 2007 are also in good agreement with those recently inferred from a diagnostic model of the ocean circulation (*21*) (fig. S6).

Table 1. Change in the inventory of anthropogenic CO_2 between 1994 and 2007 as estimated on the basis of the eMLR(C*) method. Shown in italics are the estimated uncertainties based on the sensitivity and Monte Carlo analyses.

	Atlantic (Pg C)	Pacific (Pg C)	Indian (Pg C)	Other basins† (Pg C)	Global (Pg C)
Northern Hemisphere	6.0 ± *0.4**	5.2 ± *0.6*	0.8 ± *0.4*	1.5 ± *0.6*	13.5 ± *1.0*
Southern Hemisphere	5.9 ± *1.2**	8.0 ± *1.2*	6.3 ± *3.4*	~0	20.1 ± *3.8*
Entire basin	11.9 ± *1.3*	13.2 ± *1.3*	7.1 ± *3.4*	1.5 ± *0.6*	33.7 ± *4.0*

*Includes an estimated 1 Pg C to account for the accumulation below 3000 m, with 0.7 Pg C allocated to the North Atlantic and 0.3 Pg C to the South Atlantic (see main text). †Estimated storage in the Arctic and Mediterranean Sea (see supplementary materials).

Comparison with the JGOFS-WOCE era reconstructions

The column inventory change between 1994 and 2007 (Fig. 3A) is spatially well correlated (r^2 = 0.68) with the total inventory of anthropogenic CO_2 in 1994 (Fig. 3B) (*1*). This relationship is consistent with the nearly exponential and multi-decadal nature of the anthropogenic perturbation of the global carbon cycle, which results in the establishment of a "transient steady state" (*27*). For an ocean with invariant circulation and mixing, this transient steady state implies that the change of anthropogenic CO_2 over any time period t_1 to t_2 is linearly related to the amount of anthropogenic CO_2 at the initial time, t_1, i.e., $\Delta_tC_{ant}(t_2 - t_1) \approx \alpha \cdot C_{ant}(t_1)$ (*28*). We estimate the proportionality α from theoretical considerations for the period 1994 through 2007 and obtain a value of α = 0.28 ± 0.02 (see supplementary materials). This value varies little by region, but it varies substantially over time. This theoretically estimated value is statistically indistinguishable from the ratio of the global change in inventory between 1994 and 2007 (34 ± 4 Pg C) and the inventory in 1994 (118 ± 19 Pg C). This implies that, to first order, the global ocean has continued to take up anthropogenic CO_2 from the atmosphere at a rate expected

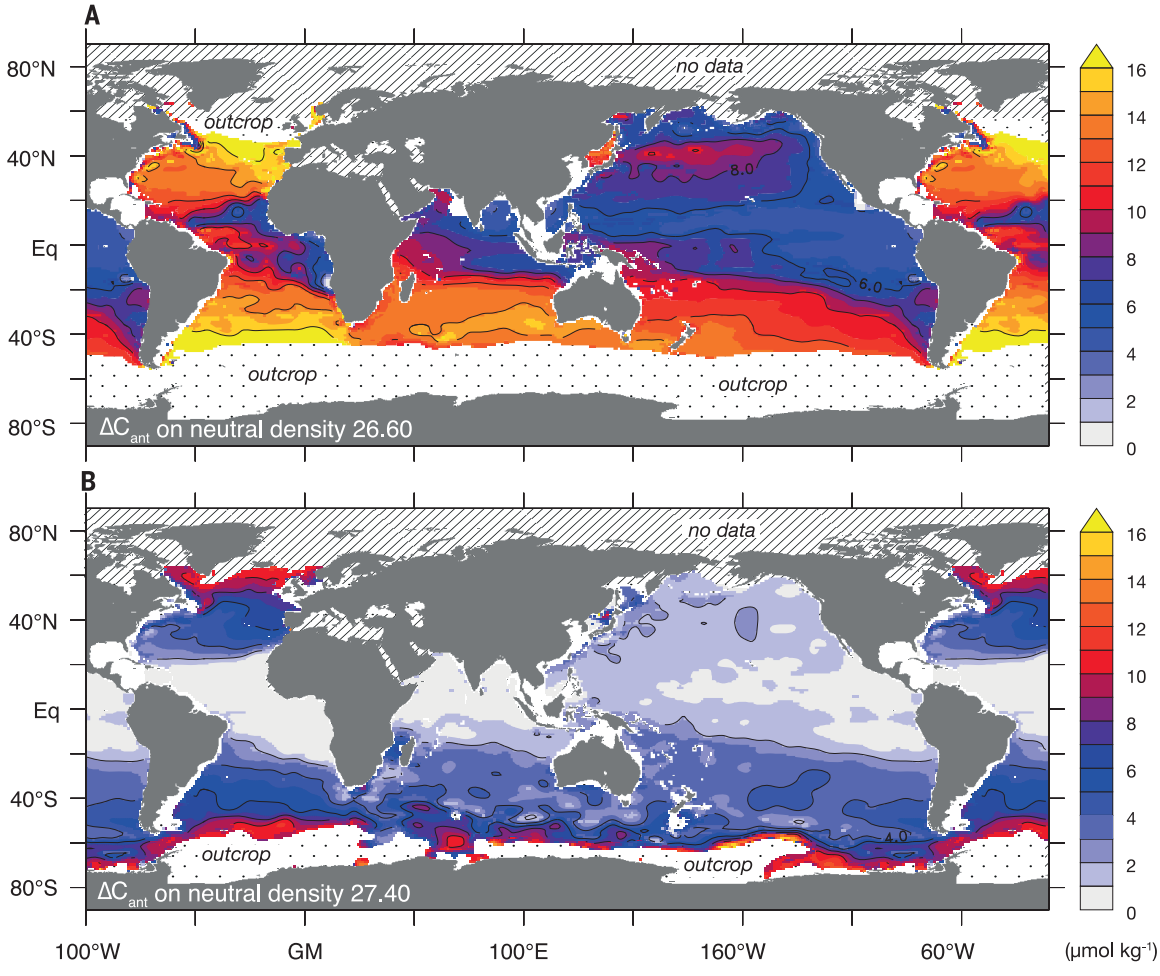

Fig. 2. Distribution of the change in anthropogenic CO_2, Δ_tC_{ant}, between 1994 and 2007 on two selected neutral surfaces. (**A**) Δ_tC_{ant} on the neutral surface 26.60 kg m^{-3}, representing subtropical mode waters and located around 400-m depth in the centers of the subtropical gyres. (**B**) Δ_tC_{ant} on the neutral surface 27.40 located at a depth of about 1000 m. In the Southern Hemisphere and in the Indian and Pacific oceans, this neutral surface represents southern-sourced Antarctic Intermediate Water, whereas in the North Atlantic it represents Intermediate Water formed in the north. Stippled areas poleward of the highest concentration of Δ_tC_{ant} indicate the outcrop areas of these neutral surfaces. Hatched areas indicate regions where no estimate of Δ_tC_{ant} was possible owing to data limitations.

from the increase in atmospheric CO_2, i.e., there is no indication of a major change in the uptake over the 1994 to 2007 period relative to the long-term mean.

On a regional basis, however, the reconstructed distribution of Δ_tC_{ant} differs from that inferred from the C_{ant} distribution in 1994 and the assumption of a transient steady state (Fig. 3C). We interpret these differences, i.e., the anomalous accumulation of C_{ant} ($\Delta_tC_{ant}^{anom} = \Delta_tC_{ant} - \alpha \cdot C_{ant}$) to be primarily the result of variations in ocean circulation. But care must be taken when interpreting $\Delta_tC_{ant}^{anom}$, because the associated uncertainties accumulate the errors from all terms, i.e., Δ_tC_{ant}, α, and C_{ant}. As shown in the supplementary materials, the most important source of error is the reconstruction of Δ_tC_{ant} itself. In particular, tests with synthetic data from an ocean biogeochemical model showed that although the eMLR(C*) method generally works well, changes in ocean circulation tend to lead to biases in the reconstructed Δ_tC_{ant}, which directly affect the inferred $\Delta_tC_{ant}^{anom}$ (*9*). However, these tests also revealed that the method is still able to recover the most important signals associated with $\Delta_tC_{ant}^{anom}$, especially in the North Atlantic. The error is largest in the North Pacific, yet across the globe, more than 50% of the modeled variance in $\Delta_tC_{ant}^{anom}$ at basin scales is correctly recovered. Globally, the bias of the recovered $\Delta_tC_{ant}^{anom}$ is essentially zero.

The most prominent anomaly is found in the North Atlantic, where the reconstructed change

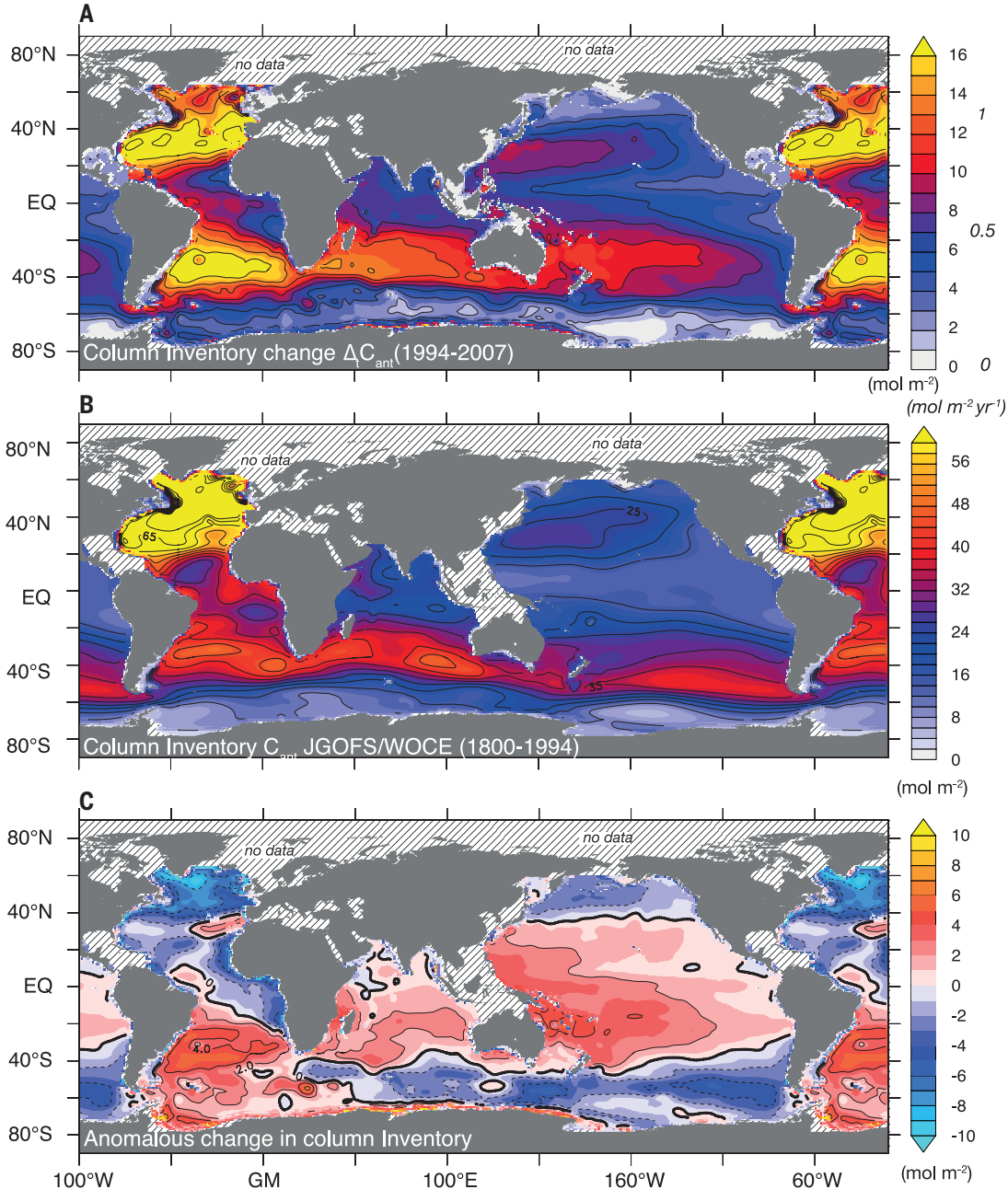

Fig. 3. Maps of the column inventories of anthropogenic CO_2 in the ocean (0 to 3000 m). (**A**) Change in column inventory between 1994 and 2007 based on the eMLR(C*) method. (**B**) Column inventory for the year 1994 (*1*) based on the ΔC* method (*45*). (**C**) Anomalous change in column inventory estimated from the difference between the change in the vertical column inventory [shown in (A)] and that expected on the basis of the transient steady-state model and the C_{ant} inventory [shown in (B)], namely, $\Delta_tC_{ant}^{anom} = \Delta_tC_{ant} - \alpha \cdot C_{ant}(1994)$, α = 0.28. The column inventories were obtained by vertically integrating the values from the surface down to 3000 m. Hatched areas indicate regions where no estimate of Δ_tC_{ant} was possible owing to data limitations.

in inventory over the entire basin is 20% smaller than that predicted by the transient steady state (Fig. 3C). This anomaly, likely robust given that it was well recovered in the tests with synthetic data, characterizes nearly the entire water column (Fig. 4A). The strongest $\Delta_t C_{ant}^{anom}$ signals are found in the subpolar gyre and within the Subpolar Mode Water and in the Intermediate Water, both belonging to the water masses with the highest burden of anthropogenic CO_2 (*10*, *29*). This lower-than-expected increase in storage in the North Atlantic during the 1990s and early 2000s has been described previously (*29*–*31*) and was attributed to the slow-down and reorganization of the North Atlantic overturning circulation at that time, which led to a reduction in the downward transport of C_{ant} (*29*, *31*). This slowdown was probably temporary, as indicated by the more recent rapid increase in C_{ant} in the Irminger Sea (*32*).

The anomalously low accumulation in the North Atlantic between 1994 and 2007 co-occurred with an anomalously high accumulation in the South Atlantic, such that the storage change of the entire Atlantic remained very close to the expected one. Even though we are somewhat less confident about the reconstructed $\Delta_t C_{ant}^{anom}$ in the South Atlantic given our tests with synthetic data (*9*), we point out that such a shift in storage from the Northern to the Southern Hemisphere was seen in previous $\Delta_t C_{ant}$ reconstructions, albeit based on a single meridional section (*30*).

A second set of major regions of anomalous change in inventory are the Indian and Pacific sectors of the Southern Ocean, where the changes in storage are about 20% lower than expected (Fig. 3C). The tests with synthetic data showed that changes in these regions should be captured by the eMLR(C*)-based reconstruction, although likely underestimated (*9*). We have some confidence in the robustness of this signal because it is caused by a negative $\Delta_t C_{ant}^{anom}$ that is confined to the neutral density layers of Antarctic Intermediate Water and found in all ocean basins (Fig. 4). We interpret this signal to be the result of the southward movement and strengthening of the westerly wind belt (*33*), which has caused large-scale coherent changes

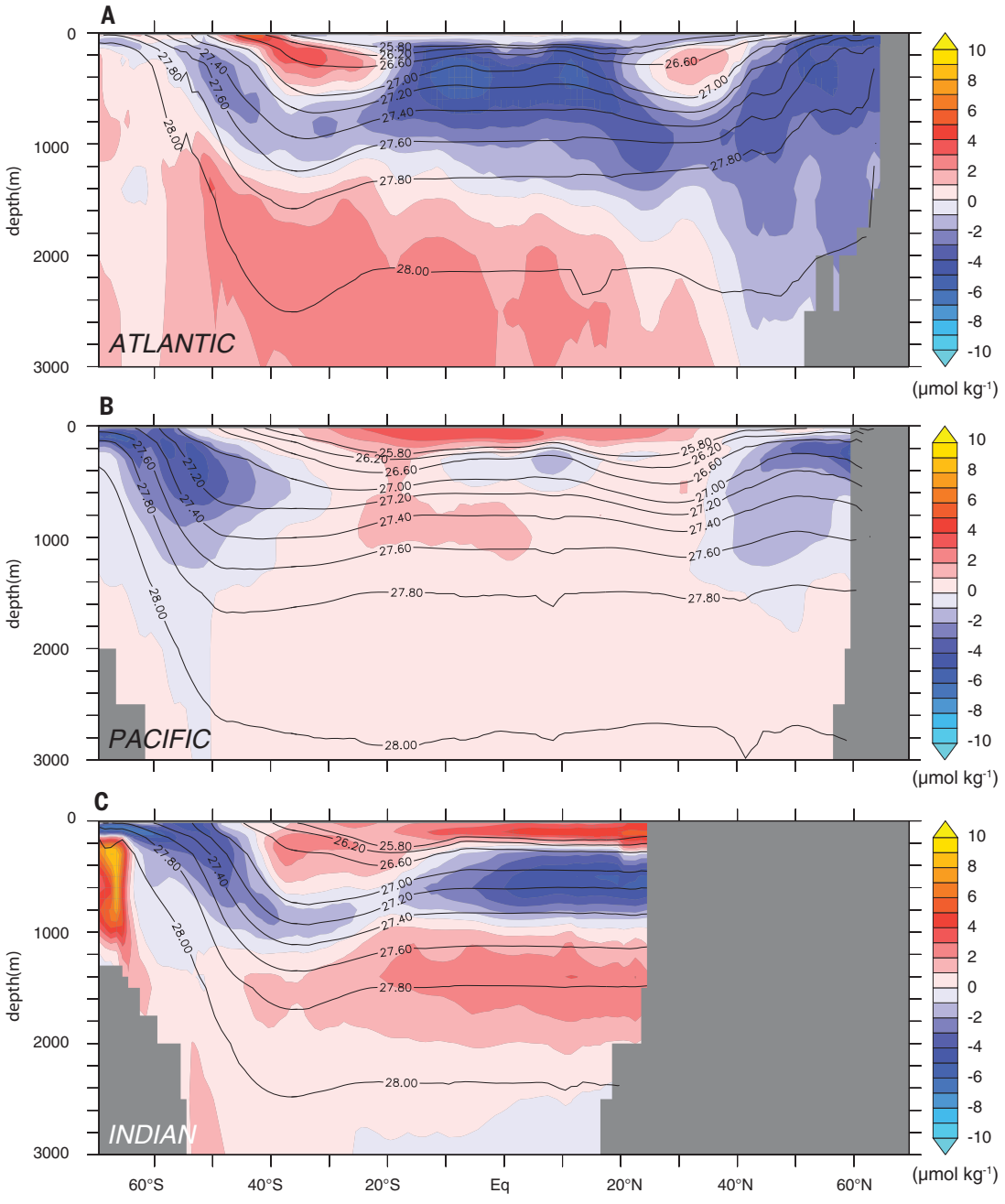

Fig. 4. Zonal mean sections of the anomalous change in C_{ant}, i.e., $\Delta_t C_{ant}^{anom} = \Delta_t C_{ant} - \alpha \cdot C_{ant}$ (1994), $\alpha = 0.28$. (**A**) Zonal mean section in the Atlantic; (**B**) as in (A), but for the Pacific; and (**C**), as in (A), but for the Indian Ocean. Selected isolines of zonally averaged neutral density are shown as contour lines in all plots.

Table 2. Global CO_2 budget for both the period 1800 to 1994 and the decadal period from 1994 to 2007. In comparison to previous budgets (*1*), we include explicitly also the potential loss of natural CO_2 from the ocean as a component of the budget. The potential contribution of changes in the land-to-ocean carbon fluxes through aquatic systems (*46*) is not considered here.

CO_2 sources and sinks	1800 to 1994 (Pg C)*	1994 to 2007 (Pg C)†
Constrained sources and sinks		
(1) Emissions of C_{ant} from fossil fuel and cement production	244 ± 20	94 ± 5‡
(2) Increase of CO_2 in the atmosphere	−165 ± 4	−50 ± 1§
(3a) Uptake of C_{ant} by the ocean	−118 ± 19	−34 ± 4‖
(3b) Loss of natural CO_2 by the ocean	7 ± 10¶	5 ± 3#
(3) Net ocean CO_2 uptake	−111 ± 21	−29 ± 5
Inferred terrestrial balance		
(4) Net terrestrial balance [−(1)−(2)−(3)]	32 ± 30	−15 ± 7
Terrestrial balance		
(5) Emissions of C_{ant} from land use change	100 to 180	16 ± 6**
(6) Terrestrial biosphere sink [−(1)−(2)−(3)] −(5)	−68 to −148	−31 ± 9

*Budget as listed in (*1*), except for 3b. †The numbers correspond to the period from mid-1994 to mid-2007. ‡Boden *et al.* (*5*). §Dlugokencky and Tans (*37*). ‖This study. ¶Keeling (*38*); Sabine and Gruber (*47*). #See text, based on Landschützer *et al*. (*39*). **Average of Houghton and Nassikas (*4*) and Hansis *et al*. (*48*).

in the meridional overturning circulation in the Southern Ocean and the ventilation of the water masses (*34*, *35*). Further, the wind changes have caused increased upwelling over the Southern Ocean and enhanced Ekman transport to the north, leading to shorter residence times of waters at the surface. This could have led to the weaker uptake and consequently weaker downward transport of anthropogenic CO_2 into the thermocline by the upper cell of the meridional overturning circulation, leading to the observed negative $\Delta_t C_{ant}^{anom}$ in the Antarctic Intermediate Water.

Additional support of our interpretation that the reconstructed $\Delta_t C_{ant}^{anom}$ are real stems from the overall agreement of our result with those inferred recently from a diagnostic ocean model (*21*). Although our changes are somewhat larger, the patterns agree well and support the conclusion that the changes primarily reflect changes in ocean circulation.

Implications

Our reconstructed changes in the oceanic inventory of anthropogenic CO_2 imply a continuing strong role of the ocean in the recent global carbon budget (Table 2). From 1994 to 2007, anthropogenic emissions added 110 ± 8 Pg C to the atmosphere (*36*), most of which stemmed from the burning of fossil fuels (94 ± 5 Pg C) (*5*). Of these emissions, 50 ± 1 Pg C (45%) remained in the atmosphere (*37*). Our uptake estimate of 34 ± 4 Pg C implies that the ocean accounts for the removal from the atmosphere of 31 ± 4% of the total anthropogenic CO_2 emissions over this time period (Table 2). This anthropogenic CO_2 uptake fraction does not differ from that for the period from preindustrial times up to 1994 (*1*).

Our ocean uptake estimate for anthropogenic CO_2 permits us also to provide a constraint on the net land uptake for the 1994 through 2007 period. This requires us to consider also the potential contribution of a small anomalous (non–steady state) net flux of natural CO_2, emerging from processes such as ocean warming and climate variability–driven changes in ocean circulation and biology (*38*). We obtain a rough estimate of this contribution by using the surface ocean partial pressure of CO_2 (pCO_2)–based air-sea flux estimate of (*39*) for the 1994 through 2007 period and subtracting from it the expected anthropogenic uptake flux consistent with (*17*), while accounting also for the steady-state outgassing of natural CO_2. This yields a cumulative anomalous net release of natural CO_2 of about 5 ± 3 Pg C. The resulting net (natural and anthropogenic CO_2) ocean uptake estimate of 29 ± 5 Pg C for the 1994 through 2007 period implies a net terrestrial biosphere sink over this period of 31 ± 9 Pg, or about 2.4 ± 0.7 Pg C $year^{-1}$ (Table 2). Our data-based net ocean uptake estimate confirms the model-based 26 ± 4 Pg C ocean sink reported by the Global Carbon Project over the 1994 through 2007 period (*36*).

Although the ~30% increase in the oceanic burden of anthropogenic CO_2 between 1994 and 2007 constitutes a great service for humanity by slowing down the accumulation of CO_2 in the atmosphere, this service comes with the cost of increased ocean acidification (*40*). Our reconstructed increases in C_{ant} imply a deep reach of ocean acidification into the ocean's interior (*41*, *42*), causing a further shoaling of the ocean's saturation horizons for biogenic carbonate minerals (*43*), and a further squeezing of the available habitats for the organisms sensitive to changes in the ocean's CO_2 chemistry (*40*, *44*).

Documenting and quantifying these changes in anthropogenic CO_2 and ocean acidification require the continuation of whole-ocean observations of inorganic carbon and of the many ancillary variables needed to produce the internally consistent data products that are so crucial for analyzing long-term changes in ocean carbon storage. In addition, the continuing documentation of the biogeochemical and physical changes in the ocean will be essential for understanding any forthcoming changes in ocean biology.

REFERENCES AND NOTES

1. C. L. Sabine *et al*., *Science* **305**, 367–371 (2004).
2. B. I. McNeil, R. J. Matear, *Biogeosciences* **10**, 2219–2228 (2013).
3. J. L. Sarmiento, J. C. Orr, U. Siegenthaler, *J. Geophys. Res.* **97** (C3), 3621–3645 (1992).
4. R. A. Houghton, A. A. Nassikas, *Global Biogeochem. Cycles* **31**, 456–472 (2017).
5. T. Boden, G. Marland, R. J. Andres, (1999): Global, Regional, and National Fossil-Fuel CO_2 Emissions (1751 - 2014) (V. 2017) (Carbon Dioxide Information Analysis Center, Oak Ridge National Laboratory, Oak Ridge, TN).
6. N. Gruber *et al*., *Global Biogeochem. Cycles* **23**, GB1005 (2009).
7. L. D. Talley *et al*., *Annu. Rev. Mar. Sci.* **8**, 185–215 (2016).
8. A. Olsen *et al*., *Earth Syst. Sci. Data* **8**, 297–323 (2016).
9. D. Clement, N. Gruber, *Global Biogeochem. Cycles* **32**, 654–679 (2018).
10. K. Friis, A. Körtzinger, J. Pätsch, D. W. R. Wallace, *Deep-Sea Res. Part I.* **52**, 681–698 (2005).
11. J. L. Sarmiento, N. Gruber, *Ocean Biogeochemical Dynamics* (Princeton Univ. Press, Princeton, NJ, 2006).
12. N. Gruber, *Global Biogeochem. Cycles* **12**, 165–191 (1998).
13. S. Khatiwala *et al*., *Biogeosciences* **10**, 2169–2191 (2013).
14. T. DeVries, *Global Biogeochem. Cycles* **28**, 631–647 (2014).
15. D. R. Jackett, T. J. McDougall, *J. Phys. Oceanogr.* **27**, 237–263 (1997).
16. K. Hanawa, L. D. Talley, in *Ocean Circulation and Climate*, G. Siedler, J. Church, Eds. (Academic Press, San Diego, 2001), pp. 373–386.
17. S. E. Mikaloff Fletcher *et al*., *Global Biogeochem. Cycles* **20**, GB2002 (2006).
18. L. Bopp, M. Lévy, L. Resplandy, J. B. Sallée, *Geophys. Res. Lett.* **42**, 6416–6423 (2015).
19. J. Marshall, K. Speer, *Nat. Geosci.* **5**, 171–180 (2012).
20. M. Hoppema, W. Roether, R. G. J. Bellerby, H. J. W. de Baar, *Geophys. Res. Lett.* **28**, 1747–1750 (2001).
21. T. DeVries, M. Holzer, F. Primeau, *Nature* **542**, 215–218 (2017).
22. A. Olsen, A. M. Omar, E. Jeansson, L. G. Anderson, R. G. J. Bellerby, *J. Geophys. Res.* **115**, C05005 (2010).
23. T. Tanhua *et al*., *J. Geophys. Res.* **114**, C01002 (2009).
24. A. Schneider, T. Tanhua, A. Körtzinger, D. W. R. Wallace, *J. Geophys. Res.* **115**, C12050 (2010).
25. R. Wanninkhof *et al*., *Deep Sea Res. Part II Top. Stud. Oceanogr.* **74**, 48–63 (2013).
26. S. Khatiwala, F. Primeau, T. Hall, *Nature* **462**, 346–349 (2009).
27. R. H. Gammon, J. Cline, D. Wisegarver, *J. Geophys. Res.* **87** (C12), 9441–9454 (1982).
28. T. Tanhua, A. Körtzinger, K. Friis, D. W. Waugh, D. W. R. Wallace, *Proc. Natl. Acad. Sci. U.S.A.* **104**, 3037–3042 (2007).
29. R. Steinfeldt, M. Rhein, J. L. Bullister, T. Tanhua, *Global Biogeochem. Cycles* **23**, GB3010 (2009).
30. R. Wanninkhof *et al*., *J. Geophys. Res.* **115**, C11028 (2010).
31. F. F. Pérez *et al*., *Nat. Geosci.* **6**, 146–152 (2013).
32. F. Fröb *et al*., *Nat. Commun.* **7**, 13244 (2016).
33. D. W. J. Thompson, S. Solomon, *Science* **296**, 895–899 (2002).
34. D. W. Waugh, F. Primeau, T. Devries, M. Holzer, *Science* **339**, 568–570 (2013).
35. T. Tanhua *et al*., *Deep-Sea. Res. Part II Top. Stud. Oceanogr.* **138**, 26–38 (2017).
36. C. Le Quéré *et al*., *Earth Syst. Sci. Data* **10**, 405–448 (2018).
37. E. Dlugokencky, P. Tans, "Trends in atmospheric carbon dioxide" (Boulder, CO, USA, 2017); www.esrl.noaa.gov/gmd/ccgg/trends/gl_data.html.
38. R. F. Keeling, *Science* **308**, 1743c (2005).
39. P. Landschützer, N. Gruber, D. C. E. Bakker, *Global Biogeochem. Cycles* **30**, 1396–1417 (2016).
40. S. C. Doney, V. J. Fabry, R. A. Feely, J. A. Kleypas, *Annu. Rev. Mar. Sci.* **1**, 169–192 (2009).

41. R. A. Feely *et al*., *Science* **305**, 362–366 (2004).
42. F. F. Perez *et al*., *Nature* **554**, 515–518 (2018).
43. B. R. Carter *et al*., *Global Biogeochem. Cycles* **31**, 306–327 (2017).
44. K. J. Kroeker, R. L. Kordas, R. N. Crim, G. G. Singh, *Ecol. Lett.* **13**, 1419–1434 (2010).
45. N. Gruber, J. L. Sarmiento, T. F. Stocker, *Global Biogeochem. Cycles* **10**, 809–837 (1996).
46. P. Regnier *et al*., *Nat. Geosci.* **6**, 597–607 (2013).
47. C. Sabine, N. Gruber, *Science* **308**, 1743c (2005).
48. E. Hansis, S. J. Davis, J. Pongratz, *Global Biogeochem. Cycles* **29**, 1230–1246 (2015).

ACKNOWLEDGMENTS

We are deeply indebted to the large number of principal investigators, scientists, and technicians who acquired the high-quality oceanographic data that made our study possible. This global synthesis is the outcome of an effort led by the joint IMBER-SOLAS Ocean carbon cycle working group 2. We acknowledge the support from the two parent organizations IMBER and SOLAS. We also thank the anonymous reviewers for their insightful and supportive input. **Funding:** We are grateful to the many funding agencies in the various countries that financially supported the global ship-based surveys that underpin much of this work. In particular, we acknowledge funding from the U.S. National Science Foundation and from the National Oceanic and Atmospheric Administration (NOAA), and the GO-SHIP program together with the International ocean carbon coordination project (IOCCP), for their efforts to initiate and coordinate the repeat hydrography program. The work of N.G. and D.C. was supported by ETH and the FP7 projects CarboChange (264879) and Geocarbon (283080). S.v.H. also received support from CarboChange (264879). R.W., R.A.F., and B.R.C. acknowledge the support of Oceanic and Atmospheric Research NOAA and the U.S. Department of Commerce, including resources from the NOAA Global Ocean Monitoring and Observations Division (fund reference 100007298). This is contribution no. 4796 from the NOAA Pacific Marine Environmental Laboratory and JISAO contribution 2018-0185. M.I. acknowledges support from the Japan Meteorological Agency and MEXT KAKENHI grant no. 24121003 "NEOPS" and JP16H01594 "OMIX". S.K.L. acknowledges support from the Research Council of Norway (214513). F.F.P. was supported by Ministerio de Economía y Competitividad through the ARIOS (CTM2016-76146-C3-1-R) project cofunded by the Fondo Europeo de Desarrollo Regional 2014-2020 (FEDER) and EU Horizon 2020 through the AtlantOS project (grant agreement 633211). **Author contributions:** N.G. led the global synthesis project together with R.W., R.A.F., T.T., M.I., and J.M. N.G. conceived and developed the eMLR(C*) method together with D.C., analyzed the results, and wrote the paper with input from all coauthors. D.C. undertook additional quality controls on the data with input from S.v.H., conducted the estimate of changes in anthropogenic CO_2 together with N.G., and supported all analyses. S.v.H. performed additional inversion of the data. A.O. led the team that conducted the secondary quality control of the GO-SHIP and JGOFS–WOC-era cruises. All authors provided expertise at all stages, were involved in the analysis and interpretation of the data, and contributed to the writing of the manuscript. **Competing interests:** The authors declare that they have no competing interests. **Data and materials availability:** The inorganic carbon observations from GLODAPv2 underlying this study are available from the GLODAP website: www.glodap.info. The anthropogenic CO_2 estimates reported in this paper can be obtained through NCEI's Ocean Carbon Data System: www.nodc.noaa.gov/ocads/index.html.

SUPPLEMENTARY MATERIALS

www.sciencemag.org/content/363/6432/1193/suppl/DC1
Supplementary Text
Figs. S1 to S10
Tables S1 to S3
References (*49*–*71*)

3 July 2018; accepted 19 February 2019
10.1126/science.aau5153

The oceanic sink for anthropogenic CO_2 from 1994 to 2007

Nicolas Gruber, Dominic Clement, Brendan R. Carter, Richard A. Feely, Steven van Heuven, Mario Hoppema, Masao Ishii, Robert M. Key, Alex Kozyr, Siv K. Lauvset, Claire Lo Monaco, Jeremy T. Mathis, Akihiko Murata, Are Olsen, Fiz F. Perez, Christopher L. Sabine, Toste Tanhua and Rik Wanninkhof

Science **363** (6432), 1193-1199.
DOI: 10.1126/science.aau5153

The state of ocean CO_2 uptake

The ocean is an important sink for anthropogenic CO_2 and has absorbed roughly 30% of our emissions between the beginning of the industrial revolution and the mid-1990s. This effect is an important moderator of climate change, but can we count on it to remain as strong in the future? Gruber *et al.* calculated the ocean uptake of anthropogenic CO_2 for the interval from 1994 to 2007, which continued as expected. They also observed clear regional deviations from this pattern, suggesting that there is no guarantee that uptake will remain as robust with time.

Science, this issue p. 1193